August 11, 2005

Measuring the Tau Pair Production Cross-Section

Adam Hinkle
Marquette University

The CLEO-c experiment can study tau physics at low energies. The Cornell Electron Storage Ring (CESR) collides electrons and positrons inside the CLEO detector. Various particles such as *u, d, s*, and *c* quarks, electrons, muons, or tau leptons are produced in the resulting annihilation. A signal for $e^+e^- \rightarrow \tau^+\tau^-$ was isolated at the ψ'' (3.770 GeV) energy range by selecting events with two tracks. A Monte Carlo program was used to simulate the various interactions and decays involved according to Standard Model branching ratios. Cuts were imposed upon the data and the Monte Carlo and the production cross section for the creation of tau pairs was determined.

I. INTRODUCTION

Prior to the completion of this project the tau pair production cross section had not been experimentally well-measured near the ψ'' center of mass energy. Production cross sections are known constants calculated from the Standard Model of elementary particles and then experimentally measured. The production cross section, $\sigma(E_{cm})$, for the creation of $\tau^+\tau^-$ is a function of the center of mass energy and has dimension of area, usually expressed in barns (b) where 1 barn is equal to $10^{-28}m^2$. Also of necessity in measuring $\sigma_{\tau\tau}$ is the luminosity, $\mathcal{L}(t)$, which is a function of time and has dimensions of number of particles produced per unit time per unit area. The luminosity integrated over all of time is needed to calculate the total number of particles produced in a given interaction. The relationship between these quantities is (where $N_{\tau\tau}$ is the number of tau pairs produced):

$$N_{\tau\tau} = \sigma_{\tau\tau} \int \mathcal{L}(t)dt \tag{1}$$

The measurement itself is a straightforward task that is complicated only by the various backgrounds which obscure the detection of tau pairs. Because $e^+e^- \rightarrow \tau^+\tau^-$ mostly involves only QED interactions, powerful Monte Carlo techniques therefore allow these backgrounds to be simulated according to their Standard Model branching ratios. The resulting measurement of the production cross section is determined by fitting the data to the Monte Carlo and correcting for the backgrounds. The number of real tau events from the data, $N_{data}^{real\tau\tau}$ is found by subtracting the sum of the expelled background events from the data, N_{data}^{realbg}, multiplied by the efficiency of the background Monte Carlo, ϵ_{MC}^{bg} from the number of events observed in the data, N_{data}^{obs}, and finally dividing by the efficiency for observing tau events, $\epsilon_{MC}^{\tau\tau}$.

$$N_{data}^{real\tau\tau} = \frac{N_{data}^{obs} - \Sigma N_{data}^{realbg}\epsilon_{MC}^{bg}}{\epsilon_{MC}^{\tau\tau}} \tag{2}$$

Equation (1) can then be solved for $\sigma_{\tau\tau}$.

$$\sigma_{\tau\tau} = N^{real\tau\tau}_{data\tau\tau} / \int \pounds(t)dt \qquad (3)$$

II. THE MONTE CARLO

The Monte Carlo program, endnote1 *KoralB*, was used to generate tau pairs produced at the charm energy range. The tau is a very short-lived particle with an average lifetime of 290 x 10^{-15} seconds. The tau decays to the final states shown below according to the corresponding branching ratios:

$$\tau \to e\nu\nu \ 18\%$$
$$\tau \to \mu\nu\nu \ 18\%$$
$$\tau \to \pi\nu\nu \ 12\%$$
$$\tau \to \rho(\to \pi\pi^0)\nu\nu \ 24\%$$

The Monte Carlo program is designed to simulate the response of the CLEO-c detector from the input of various parameters including the beam energy and the physical properties of the detector. Using the known physics for e^+e^- interactions, the following processes were also generated:

$$e^+e^- \to \psi'', \psi'' \to D^0\overline{D^0}, D^+D^-$$
$$e^+e^- \to \gamma\psi'$$
$$e^+e^- \to q\overline{q}(u\overline{u}, d\overline{d}, s\overline{s})$$

III. ANALYSIS

The $\tau\tau$, *DD, Continuum,* and *radiative return* Monte Carlo corresponding to the decays shown above were generated with the $\tau\tau$ MC constituting the signal and the *DD, Continuum,* and *radiative return* Monte Carlos serving as the primary estimators of background in this measurement. Once this had been completed, a program was written to begin the process of isolating and subsequently removing various events from the Monte Carlo which were not the $\tau\tau$ signal. Lastly these same cuts would be applied to the data sets. The task was complicated by the fact the τ decays extremely quickly into the different particles as previously described. The CLEO detector therefore, records only these final-state particles and it is left to the experimenters to determine if they are in fact the daughters of $\tau\tau$ pairs.

The initial cuts were designed to skim through the data and eliminate events which have no relevance to the measurement being made here. This makes it much easier to separate tau events from the background assumed in the Monte Carlo. These initial skims included: eliminating events that did not have exactly two tracks, due to the fact that tau pairs decay to two charged tracks very often, while background events do so much less often. To remove Bhabha events ($e^+e^- \to e^+e^-$) each track was initially required to have momentum less than $0.95E_b$. More specific cuts took the form of cutting on other quantities. For instance it is well known that tau decays always involve neutrinos which carry away momentum and energy. Therefore a cut was made on events which possessed an angle of 180 degrees between them. This accolinearity cut seeks to eliminate Bhabha and mu pair events which have tracks that are back-to-back because they do not involve neutrinos and consequently conserve momentum and energy.

In a similar fashion a cut, "PMisCos", was placed on the direction of the missing momentum relative to the beam axis. Events such as $q\bar{q}$ can carry away momentum in the direction of the beam, and thus mimic the effects of a neutrino. Therefore, events with missing momentum pointing down the beam line were cut. Momentum in the x-y plane (the plane perpendicular to the beam) is conserved. A cut, "Pperp", was placed on the total momentum of all charged tracks orthogonal to the beam line. This was done because if neutrinos carried away momentum, the total reconstructed momentum vector would not be null. Additional cuts were imposed on the total energy of charged tracks, "Eqtot",and the total energy of neutral tracks, "Entot", to cut events from the background.

The values of all cuts were systematically varied until an optimized signal to noise ratio was reached. Histograms were then created. They recorded the number of events passing the imposed cuts with respect to each quantity upon which the cut was made. Below are the histograms for the various quantities showing the $\tau\tau$, *DD*, *Continuum*, and *radiative returns* Monte Carlo superimposed with a plot of the Sum of the MC and the real data. The *tau, DD, continuum, and radiative return* Monte Carlo sets were originally scaled to the luminosity of the data by the following factors: 0.1898, 0.0558, 0.1728, 0.1735, respectively. The resulting histograms are shown in the figures below with the data drawn in black, the *tau MC* in red, the *DD MC* in Blue, the *Continuum MC* in yellow, the radiative return MC in red, and the sum of all monte carlo sets in cyan.

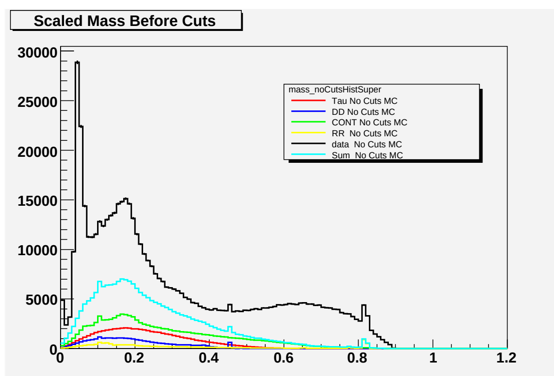

FIG. 1: Number of events vs. mass scaled to center of mass energy (E_{cm}) BEFORE any cuts. Note $D \rightarrow K\pi$ at 0.45 GeV and $\gamma\psi' \rightarrow \psi$ at 0.8 GeV. Also shown is an unknown source of background for mass less than 0.1 GeV.

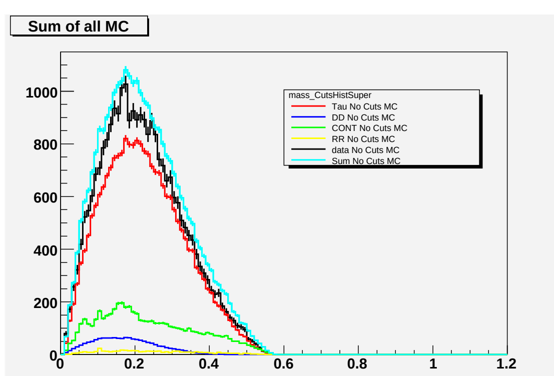

FIG. 2: Number of events vs. E_{cm} scaled mass after ALL cuts.

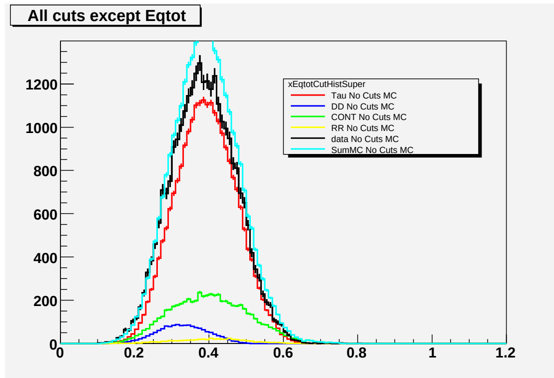

FIG. 3: Number of events vs. total charged energy (GeV) with all cuts applied except the Total Energy

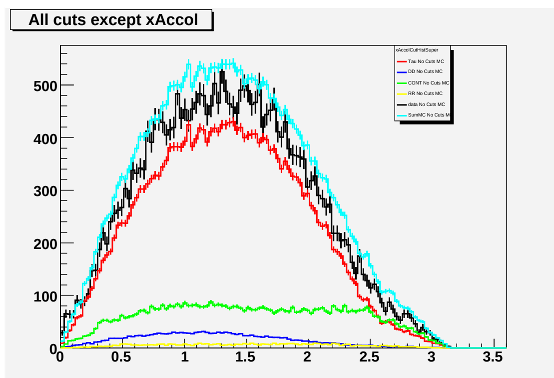

FIG. 4: Number of events vs. Accolinearity (rad) with all cuts applied except the Accolinearity

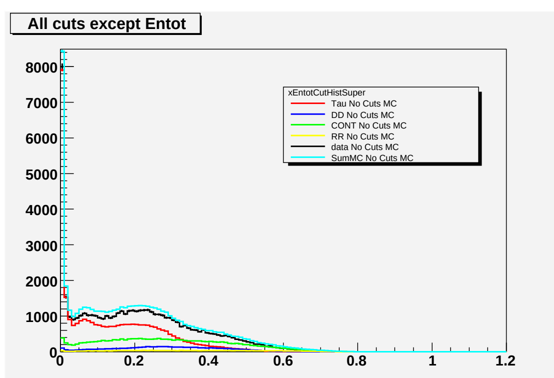

FIG. 5: Number of events vs. total neutral energy (GeV)with all cuts applied except the total neutral energy of the tracks

Cuts on the above quantities were varied systematically in order to produce a signal to noise (background events) ratio, S/N expressing the relative purity of the sample with respect to the expected backgrounds in the Monte Carlo samples by looking at the invariant mass of the two track combinations. Ideally the cuts chosen should be those which give the highest S/N. One background that was definitely not taken into account by the Monte

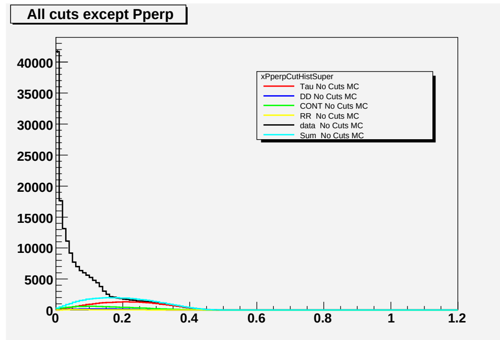

FIG. 6: Number of events vs. Pperp with all cuts applied except the Pperp. This cut is significant because of the large amount of background removed when the value of Pperp ≤ 0.2 , for which the present Monte Carlo sets do not account.

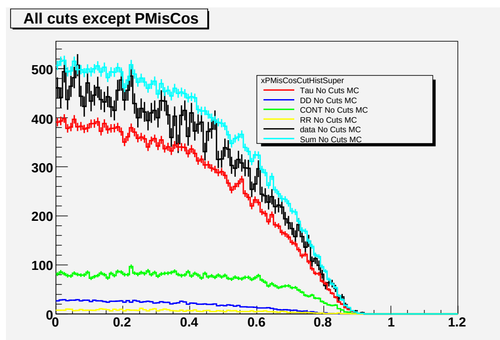

FIG. 7: Number of events vs. PMisCos (cosine of the missing momentum) with all cuts applied except PMisCos.

Carlo samples is that which produced the low Pperp discrepancy in the above figures. The source of this background is most likely $e^+e^- \to l^+l^-\gamma\gamma$, and is removed by rejecting events with low Pperp. Table I gives the cuts chosen.

TABLE I: Selected cut values.

Pperp	Min-Max Accolinearity	Eqtot	Entot	PMisCos
> 0.18	(0.1,2.75)	(0.1,0.6)	< 0.6	< 1.0

Further cuts were later imposed which allowed for the identification of the various final state particles, namely kaons, muons, electrons and pions. The particle identification histograms were primarily constructed to check on the consistency of the cross section among all τ decay modes. Particle identification used the Calorimeter, the RICH (Ring Imaging Cherenkov) and dE/dx in the tracking chamber. These cuts were chosen for expediency on the basis of previous experience.

Kaons are relatively rare in tau decays, but abundant in D decays. Thus to ensure purity, particles were tested against the Kaon hypothesis first. Kaons were identified with the RICH (Ring Imaging Cherenkov) detector if information from it was available. Because particles travel faster than the speed of light through its material, they produce a shock wave of light called Cherenkov radiation. This radiation is emitted in a conical pattern whose angle depends of the species of the particle and its energy. If the track in question was more consistent with the Kaon hypothesis, it was identified as a Kaon. Also used in Kaon identification is the rate of energy lost with respect to the particle's track length, dE/dx. Different particle species tend to leave different amounts of energy per unit path length in the drift chamber.

Since muons and pions have similar masses, dE/dx and RICH information are not expected to be very helpful in distinguishing them. Muons were simply identified as particles that deposited somewhere between 100 and 600 MeV of energy in the Calorimeter - this selection suffers from a large background due to real pions. This background should be reasonably well simulated in the Monte Carlo. This cut should be highly efficient for seeing Muons.

Electrons were identified by tracks which have a ratio of $E_{cal}/p \sim 1$, where E_{cal} is the energy deposited into the calorimeter and p is the momentum of the particle. If the mass of the electron is assumed to be nearly zero and c=1, then the relativistic four-vector, $E^2 - (pc)^2 = (mc^2)^2$, shows that this ratio should be near unity for electrons which deposit all of their energy into the calorimeter. Thus, selecting $E/p \sim 1$ enhances the number of electrons relative to pions.

Particles which were not identified as being kaons, muons or electrons, and were consistent with being pions according to the RICH and dE/dx were identified as pions.

Selected histograms of this sort are shown below with the momentum of the tag (faster) track plotted as the independent quantity. The faster track is referred to as the tag and the slower, the signal.

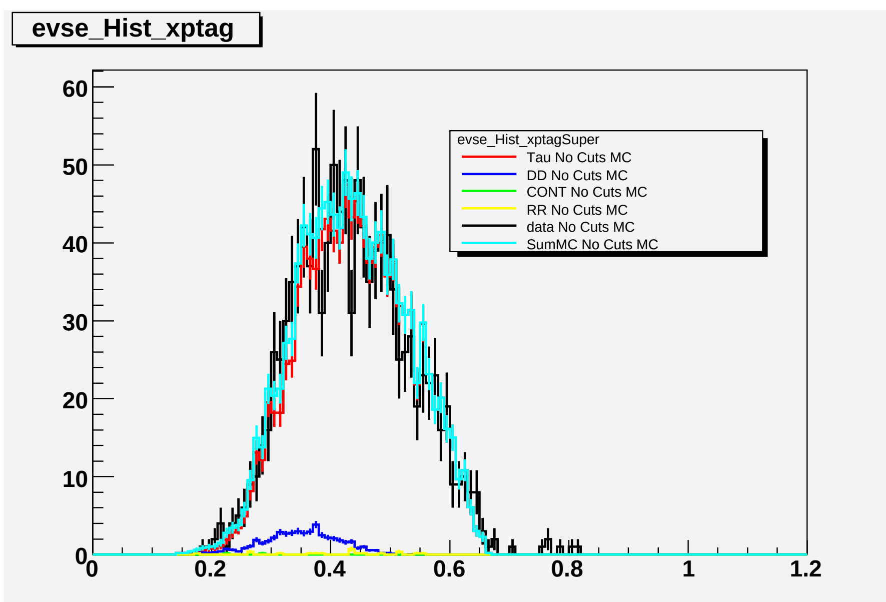

FIG. 8: Number of e^+e^- with respect to tag momentum. This histogram shows the best match of Monte Carlo to the data. In particular, there is a very large number of tau pairs indicated here which decay to e^+e^-. The number of background events are also very small here.

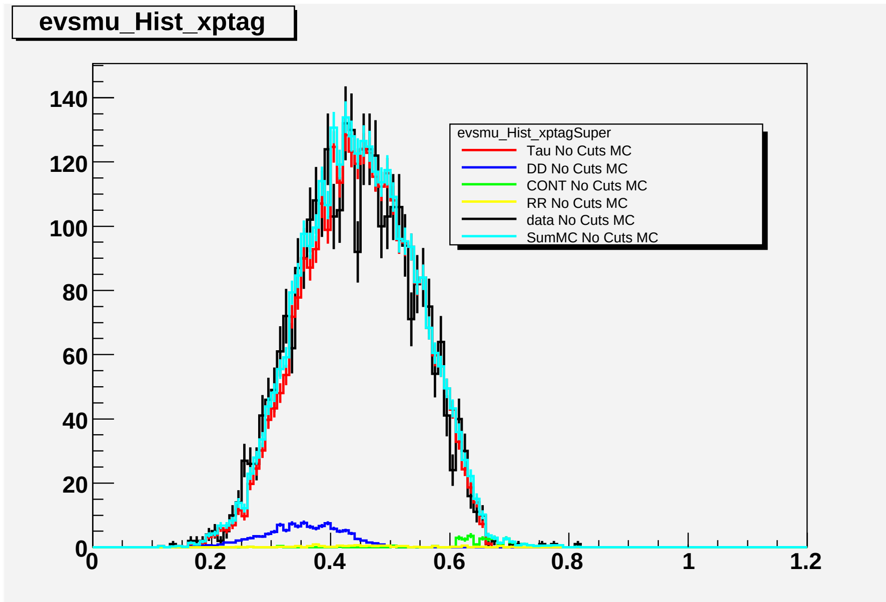

FIG. 9: Number of $e^+\mu^-$ with respect to tag momentum. A very good match of Monte Carlo to data is seen here. The background here is also very small and tau decays are very high

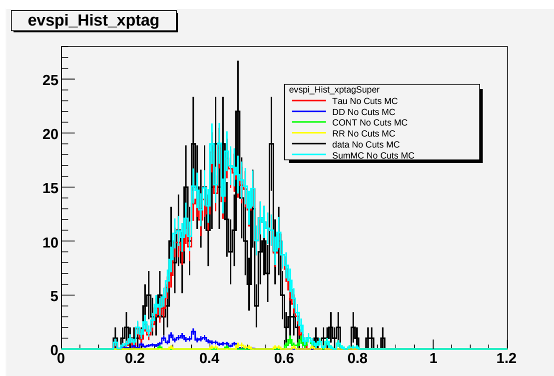

FIG. 10: Number of $e^+\pi^-$ with respect to tag momentum. This is similar to the above events, but there appears to be fewer tau decays relative to background.

IV. RESULTS FROM FITTING TAU MONTE CARLO TO DATA

After selecting the optimal cut values and studying the corresponding superimposed histograms, a program, *Minfit*, was used to fit the tau Monte Carlo to the data, while holding the *DD, continuum,* and *radiative return* Monte Carlo fixed at the original scaling factors calculated from their expected cross sections. *Minfit* performed a χ^2 fit. This determined a new scaling factor which is a measure of the fit of the tau Monte Carlo to the data. This new scaling factor was compared to the original scale factor for the tau MC which was calculated from expected values. The best fits came from the lepton verses lepton track histograms, most notably, the electron vs. muon and the muon vs. muon plots both of which show a very large number of tau events with a small number of background events. Eight fitted plots are shown. The fitted tau MC is drawn with dots, the data with error bars, and the

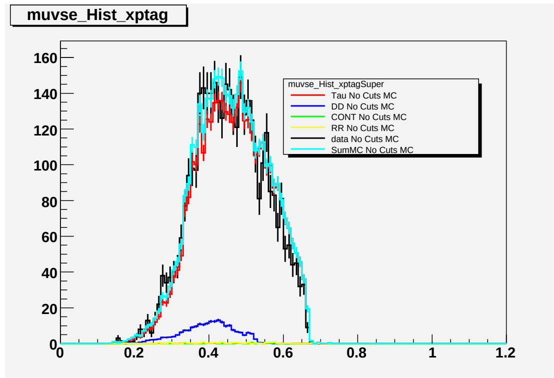

FIG. 11: Number of μ^+e^- with respect to tag momentum. A very good match of Monte Carlo to data is seen here. The background here is also very small and tau decays very high. Very few continuum events occur.

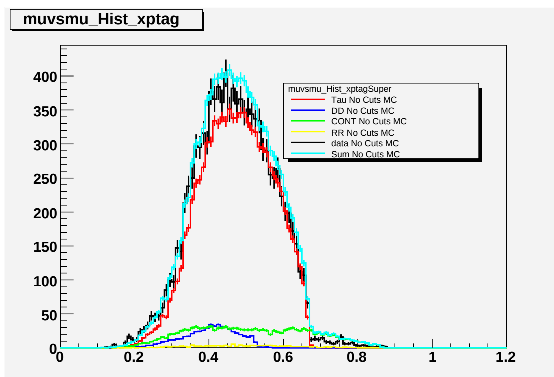

FIG. 12: Number of $\mu^+\mu^-$ with respect to tag momentum. A very good match of Monte Carlo to data is seen here. The background here is also very small and tau decays are very high.

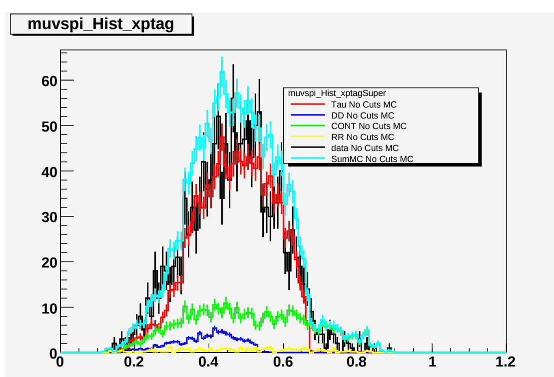

FIG. 13: Number of $\mu^+\pi^-$ with respect to tag momentum. This is similar to the above events, but there appears to be fewer tau decays relative to background.

expelled backgrounds with light dots. Their shapes and relative sizes are comparable to the previously unfit histograms.

The new scaling factors from *Minfit* are shown for each histogram with the corresponding

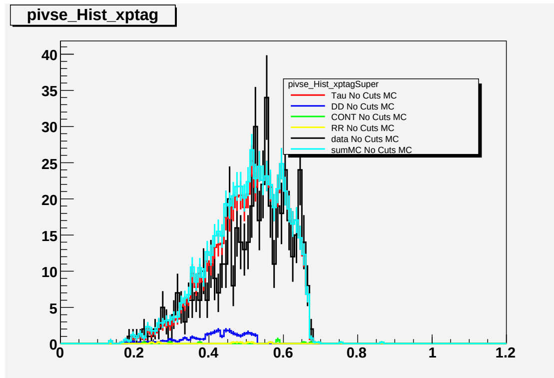

FIG. 14: Number of π^+e^- with respect to tag momentum. A very good match of Monte Carlo to data is seen here. The background here is also very small and tau decays are very high.

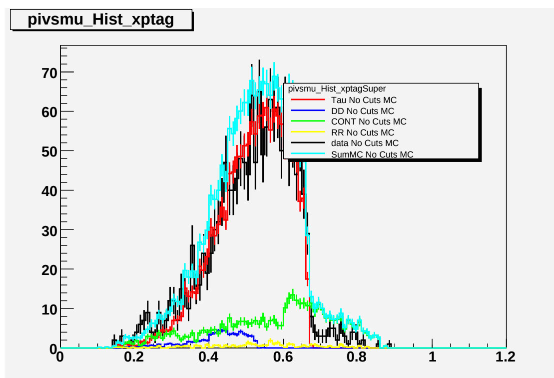

FIG. 15: Number of $\pi^+\mu^-$ with respect to tag momentum. A very good match of Monte Carlo to data is seen here. The background here is also very small and tau decays are very high.

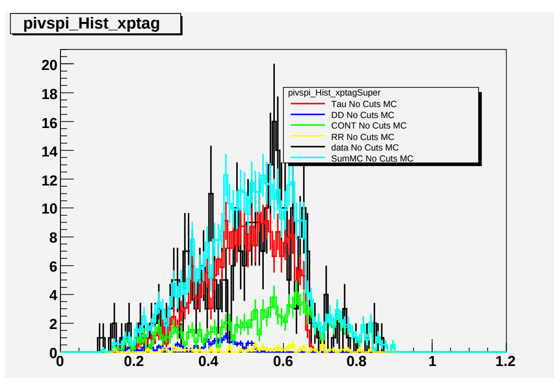

FIG. 16: Number of $\pi^+\pi^-$ with respect to tag momentum. A very good match of Monte Carlo to data is seen here. The background here is also very small and tau decays are very high.

Minfit error bars. The original scaling factor based on the Standard Model for the tau Monte Carlo was 0.1898.

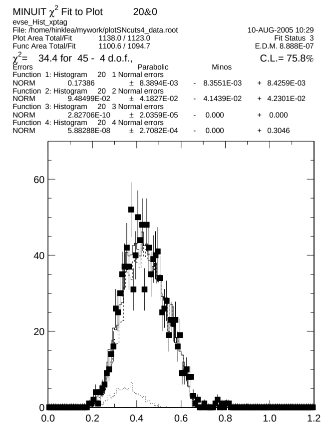

FIG. 17: Best fit of $e^{+} vs. e^{-}$ with respect to tag momentum.

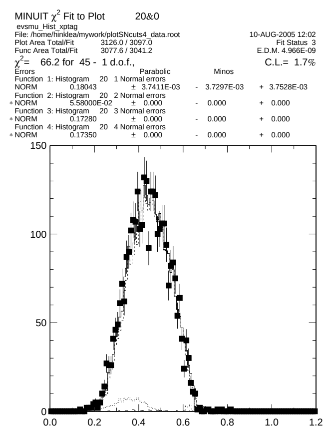

FIG. 18: Best fit of $e^{+} vs. \mu^{-}$ with respect to tag momentum.

TABLE II:

Histogram Event	Fitted-Scaling Factor	Error
e vs. e	0.1739	0.0084
e vs. μ	0.1804	0.0037
e vs. π	0.1501	0.0092
μ vs. e	0.1825	0.0036
μ vs. μ	0.1755	0.0024
μ vs. π	0.1397	0.0063
π vs. e	0.1439	0.0078
π vs. μ	0.1467	0.0055
π vs. K	2.711E-19	5.3E-11

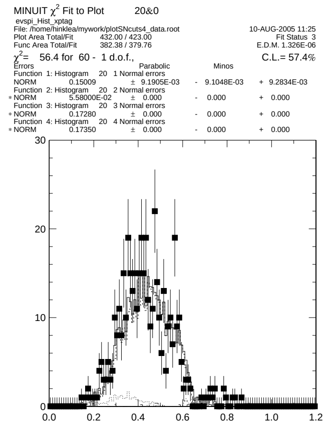

FIG. 19: Best fit of $e^+ vs. \pi^-$ with respect to tag momentum.

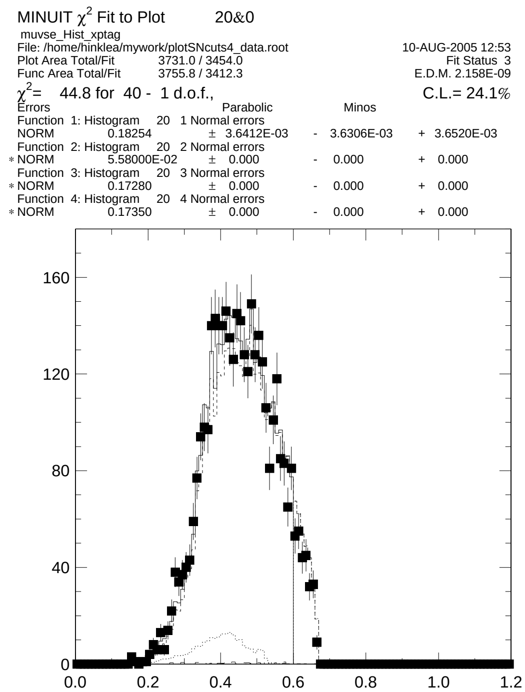

FIG. 20: Best fit of $\mu^+ vs. e^-$ with respect to tag momentum.

Finally the tau pair production cross section was determined by scaling the ratio of the fitted histogram scaled back relative to its prediction.

The measured value is : $\sigma_{\tau\tau}$ (E_{cm} = 3.77 GeV) = 2.626 ± 0.029 ± 0.103 nb. This value is somewhat lower than, but in reasonable agreement with, the Standard Model expectation derived from KoralB of 2.8 nb.

The systematic error of 0.103 is determined by examining the difference in cross sections between the lepton pair histograms and the pion-lepton histograms. It is not meant as an exhaustive systematic error but provides some measure of the scale of our error.

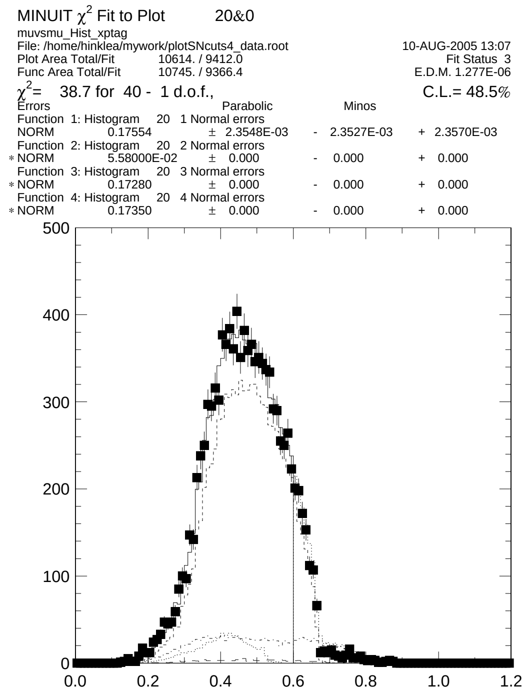

FIG. 21: Best fit of $\mu^+ vs. \mu^-$ with respect to tag momentum.

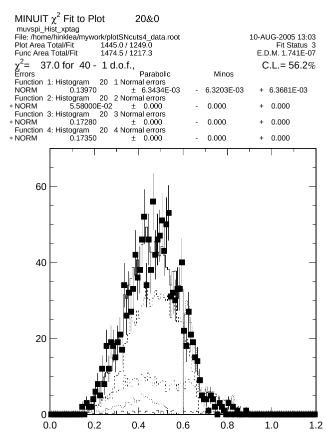

FIG. 22: Best fit of$\mu^+ vs. \pi^-$ with respect to tag momentum.

V. ACKNOWLEDGMENTS

I gratefully acknowledge Jean Duboscq of Cornell University, without whose kind support and encouragement this project would not have been possible. I am amazed at how much I have learned from him about experimental particle physics. My work this summer has been a wonderful experience for which I am immensely grateful. I also owe much thanks to David Kreinick of Cornell with whom I had many lively and helpful discussions. Peter Onyisi and Brian Heltsley, both of Cornell, graciously assisted me with their spectacular computer skills. Finally I am pleased to thank Rich Galik, principal investigator for the National Science Foundation, for his organization of the Cornell REU program at the Laboratory for Elementary Particle Physics. This experience has profoundly enriched my career as an

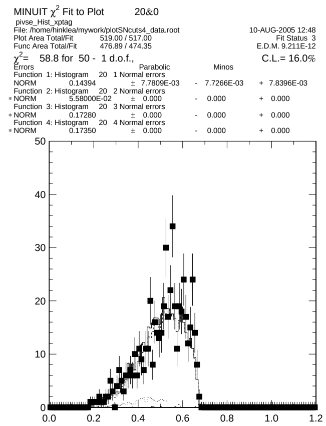

FIG. 23: Best fit of $\pi^+ vs. e^-$ with respect to tag momentum.

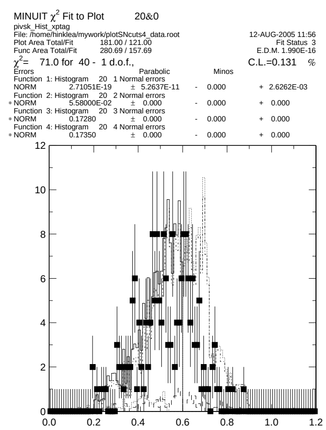

FIG. 24: Best fit of $\pi^+ vs. \mu^-$ with respect to tag momentum.

undergraduate. This work was generously supported by the National Science Foundation REU grant PHY-0243687 research co-operative agreement PHY-9809799.

NOTES

[1] S. Jadach and Z. Was, Comput. Phys. Commun. 36, 191 (1985); 64, 267 (1991); S. Jadach, J.H. Kuhn, and Z. Was, *ibid.* 64, 275 (1991).

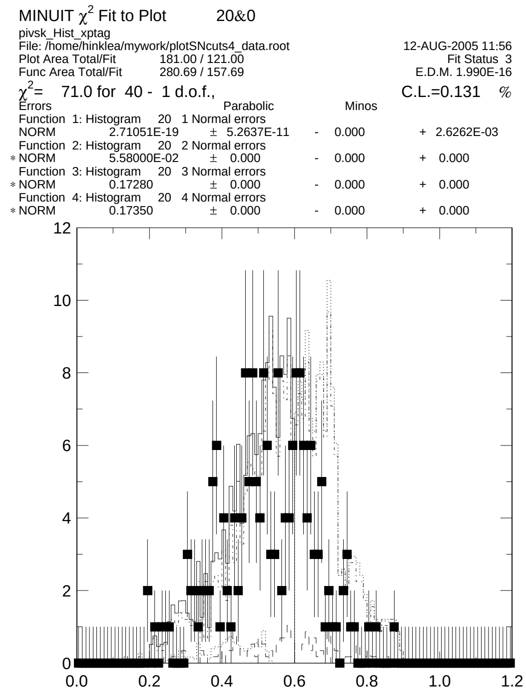

FIG. 25: Best fit of $\pi^+ vs.k^-$ with respect to tag momentum. This is a very poor fit. Very few tau events and a large number of background events are shown. This indicates that the tau rarely decays to kaons. This histogram was NOT included in the above eight when the cross-section was determined.